Molecular Basis for Jagged-1/Serrate Ligand Recognition by the Notch Receptor[*]

Pat Whiteman[‡1], Beatriz Hernandez de Madrid[§1], Paul Taylor[‡1], Demin Li[¶], Rebecca Heslop[‡], Nattnee Viticheep[‡], Joyce Zi Tan[‖], Hideyuki Shimizu[§], Juliana Callaghan[‡], Massimo Masiero[¶**], Ji Liang Li[**], Alison H. Banham[¶], Adrian L. Harris[**], Susan M. Lea[‖], Christina Redfield[‡], Martin Baron[§], and Penny A. Handford[‡2]

From the ‡Department of Biochemistry, University of Oxford, South Parks Road, Oxford OX1 3QU, the §Faculty of Life Sciences, University of Manchester, Manchester M13 9PT, the ‖Sir William Dunn School of Pathology, University of Oxford, South Parks Road, Oxford OX1 3RE, the ¶Nuffield Department of Clinical Laboratory Sciences, Oxford National Institute for Health Research (NIHR) Biomedical Research Centre, John Radcliffe Hospital, University of Oxford, Headington, Oxford OX3 9DU, and the **Molecular Oncology Laboratories, Oxford University Department of Oncology, Weatherall Institute of Molecular Medicine, John Radcliffe Hospital, University of Oxford, Oxford OX3 9DS, United Kingdom

Background: The site of Jagged/Serrate ligand recognition by Notch is unknown.
Results: Two critical residues involved in an intramolecular hydrophobic interaction across the central β-sheet of EGF_{12} form a ligand-binding platform.
Conclusion: The ligand-binding region is adjacent to a Fringe-sensitive residue involved in modulating Notch activity.
Significance: The results have implications for understanding receptor/ligand recognition, Notch regulation by O-glycosylation, and the development of paralogue-specific antibodies.

We have mapped a Jagged/Serrate-binding site to specific residues within the 12th EGF domain of human and *Drosophila* Notch. Two critical residues, involved in a hydrophobic interaction, provide a ligand-binding platform and are adjacent to a Fringe-sensitive residue that modulates Notch activity. Our data suggest that small variations within the binding site fine-tune ligand specificity, which may explain the observed sequence heterogeneity in mammalian Notch paralogues, and should allow the development of paralogue-specific ligand-blocking antibodies. As a proof of principle, we have generated a Notch-1-specific monoclonal antibody that blocks binding, thus paving the way for antibody tools for research and therapeutic applications.

The Notch receptor mediates a critical short range signal that is deployed in many developmental and adult contexts to refine cell fate choices (1). Genetic diseases affecting Notch pathway components give rise to a wide range of congenital and adult-onset disorders, and Notch dysregulation has been found to contribute to many types of human cancer (2). The Notch receptor is a single pass trans-membrane protein that, during its biosynthetic pathway, may be cleaved by a furin-like convertase (S1) in the trans-Golgi to generate a noncovalently associated heterodimer at the cell surface (3, 4). Canonical Notch signaling is initiated when a cell surface-expressed Delta/

Serrate/LAG-2 (DSL)[3] ligand binds in trans to the Notch receptor expressed on an opposing cell surface (5). Various studies have localized the binding determinants to EGF_{11-12} of the receptor and the DSL and EGF_{1-2} of the ligands (6, 7). Endocytosis of the Notch ligand complex by the ligand-expressing cell leads to a second proteolytic cleavage event at S2, which removes the extracellular moiety of the heterodimer (8). This leaves the membrane-tethered stalk, which is then cleaved by γ-secretase at S3 (see Fig. 1a) (9, 10). Following this proteolysis event, an intracellular fragment of Notch is released (11, 12). This translocates to the nucleus and assembles into a transcriptional activation complex, which includes a DNA-binding protein of the CBF-1/Suppressor of Hairless/LAG-1 (CSL) family and its co-activator Mastermind. This new assembly relieves repression and activates Notch target genes such as Hairy/Enhancer of split (*Hes*) (13).

We have previously shown that the 12th EGF (EGF_{12}) domain of Notch is directly implicated in ligand binding (14), To investigate this region further, we have made a series of single amino acid substitutions in human and *Drosophila* Notch designed to probe ligand recognition, while retaining Notch calcium binding, which is already known to be critical for this interaction (15).Using flow cytometry and cell aggregation assays, we have identified a globally conserved hydrophobic binding site that is adjacent to the residue that forms part of the O-fucosylation consensus sequence (C^2-X_4-(S/T)-C^3) in EGF_{12}, where C^2 and C^3 represent the second and third conserved cysteines (16). This residue is reported to be subjected to further modification by the Fringe enzymes (17), resulting in changes to Notch activity (18). We discuss the functional significance of sequence variability within this region and show

---

[3] The abbreviations used are: DSL, Delta/Serrate/LAG-2; J-1, Jagged-1; N-1, Notch-1; hN-1, human Notch-1; dN, *Drosophila* Notch; hNotch, human Notch.

that it can be exploited to raise paralogue-specific antibodies that block ligand binding.

EXPERIMENTAL PROCEDURES

Protein Production—hN-1_{11-13} was bacterially expressed and refolded *in vitro* as described previously and contains a 17-amino acid biotin ligase (Bir A) tag at the C terminus, which was shown to increase the efficiency of refolding (19). Calcium binding by hN-1_{11-13} wild type and mutants was measured by one-dimensional and two-dimensional NOE NMR spectroscopy, as described previously (20, 21).

Flow Cytometry of J-1/N-1 Interaction—Prokaryotically expressed and biotinylated hN-1_{11-13} wild-type and mutant constructs were coupled to purple fluorescent avidin-coated beads (Spherotech), as described previously (14). A negative control of calcium-binding EGF$_{12-14}$ from human fibrillin-1, an unrelated protein with a similar domain organization, was used in all experiments. Coupled beads were washed with 100 μl of HBSS/BSA (Hanks' buffered saline solution without phenol red, 1% BSA), resuspended in 50 μl of HBSS, 10% fetal calf serum (FCS) and kept on ice before being incubated with the cells. Stably transfected B16 mouse melanoma cells expressing full-length mouse Jagged-1 (J-1) were grown in T75 flasks to 80–90% confluency before being detached with 5 ml of PBS, 10 mM EDTA at 37 °C for 5 min. Pelleted cells from each flask were washed three times and resuspended in 1 ml of ice-cold HBSS, 10% FCS. After 1 h, 50 μl of the beads were added to 50 μl of cells and incubated on ice for 1 h prior to being resuspended in 500 μl of ice-cold HBSS for flow cytometry analysis. hN-1-binding antibodies (see below) were screened for their ability to block binding of hN-1_{11-13} to HEK293 cells expressing full-length human J-1 by the addition of 10 μl of hybridoma supernatant to the coupled beads prior to incubation with cells. Flow cytometry was performed using a FACSCalibur machine (BD Biosciences). 10,000 cells were counted, and fluorescence intensity was monitored in FL3 at >670 nm, with excitation at 488 nm.

Drosophila Cell Aggregation Assay—For Serrate expression, the 4.2-kb cDNA sequence from pBKS+SerFL (22) was amplified by PCR to eliminate the stop codon, fused in-frame to a V5-His tag at its C terminus, and inserted into the pMT expression vector (23) to generate pMT Ser-V5. Schneider S2 cells (Invitrogen) were transfected with pMT-Ser-V5 as described previously (15). Expression was induced with 1 mM CuSO$_4$ at 48 h after transfection. After a further 16 h, cells were mixed with Notch-expressing cells. For Notch expression, S2 cells were transfected with pCaSper-HS Notch (19). Expression was induced after 48 h by heat shock at 37 °C for 40 min and, after a further 4 h at 25 °C, they were mixed with wild-type Ser-V5 cells in 1.5-ml Eppendorf tubes on a rotating platform at room temperature for 30 min. The cell suspension was then transferred to coverslips coated in 0.1% poly-L-Lysine (Sigma), fixed with 2% formaldehyde, PBS for 40 min, and permeabilized with 0.2% Triton X-100, PBS for 15 min. Cells were blocked for 1 h in 0.2% Triton X-100, PBS, 5% skimmed milk powder (Sigma-Aldrich) and immunostained for 90 min with rabbit anti-V5 (Bethyl Laboratories, 1:1000) and anti-Notch C17.9C6 (Developmental Studies Hybridoma Bank, Iowa City, IA, 1:500). Secondary anti-

bodies were α-mouse-FITC (Jackson ImmunoResearch Laboratories, 1:100) and α-rabbit Cy3 (Jackson ImmunoResearch Laboratories, 1:150). Slides were imaged at ×63 with a Zeiss M2 fluorescence microscope and cooled digital camera (Orca-ER Hamamatsu), and processed using Openlab (Improvision) and Photoshop (Adobe) on an Apple Macintosh computer. Images displayed were obtained by deconvolution using the three nearest neighbors from optical sections obtained with a Z spacing of 0.5 μm. Aggregation was scored for the percentage of Notch-expressing cells adhering to at least one Serrate-expressing cell, and the mean percentage of aggregation was obtained from at least three independent transfections. Statistical significance was assessed using Student's *t* test.

Drosophila Notch Signaling—Full-length *Drosophila* Notch (dN) and L504A constructs were subcloned into pMT vectors (Invitrogen). S2 cells in 12-well dishes were transfected with pMT plasmids, Notch Response Element (NRE):Firefly (gift from S. Bray), and actin:*Renilla* (gift from G. Merdes). After 24 h, cells were resuspended and seeded into white 96-well plates (Nunc 136101), and CuSO$_4$ was added after a further 24 h to induce expression. Cells were reseeded into white 96-well plates on top of fixed Delta-expressing S2 cells (S2-Mt-Dl; *Drosophila* Genomics Resource Center (DGRC)). 24 h after induction, luciferase activity was assayed with Dual-Glo Luciferase (Promega) and quantified by luminometer (Berthold Technologies), and the Firefly/*Renilla* ratio was calculated for triplicate samples. Experiments were repeated a minimum of three times.

mAb Generation and Validation—Mouse monoclonal antibodies (N1-96A, isotype IgG2a and N1-39E, isotype IgG1) were raised, using MF1 mice and NS0 cells as the fusion partner (24). The antigen was bacterially expressed recombinant hN-1_{11-13} as described above, using TiterMax Gold as adjuvant. Fifteen hybridoma cell lines, generated from three fusions, were positive for antibody reactivity against hN-1_{11-13} by ELISA assay against the immunogen. Two hybridoma lines (N1-39E and N1-96A) were found to be positive for the detection of cell surface N-1 by FACS analysis of transient HEK293T transfectants. For epitope mapping, wild-type and mutant hN-1_{11-13} constructs were prepared at 20 ng/μl, and 1 μl of each was spotted onto nitrocellulose. The proteins were detected with the noninhibitory antibody N1-96A (1:200) and the blocking antibody N1-39E (1:400) followed by anti-mouse HRP conjugate (1:2000) and visualized by chemiluminescence (Amersham Biosciences ECL Plus Western blotting detection system).

Flow Cytometry and Immunocytochemistry to Test Paralogue Specificity—Full-length human Notch-1, -2, -3, and -4 transiently transfected HEK293T cells were generated. Cells were washed three times with FACS Wash Buffer (2% FBS in PBS + 0.01% NaN3) and then incubated on ice for 20 min with primary antibody, *i.e.* undiluted hybridoma supernatant. After two washes with FACS Wash Buffer, cells were incubated for 20 min at 4 °C (protected from light) with secondary conjugated antibody, *i.e.* allophycocyanin-conjugated anti-mouse Ig (H+L) (Invitrogen, A10539) at 1:50 dilution. Cells were washed with FACS Wash Buffer and resuspended in 500 μl of 1% formaldehyde in PBS before analysis using a FACSCalibur flow cytome-
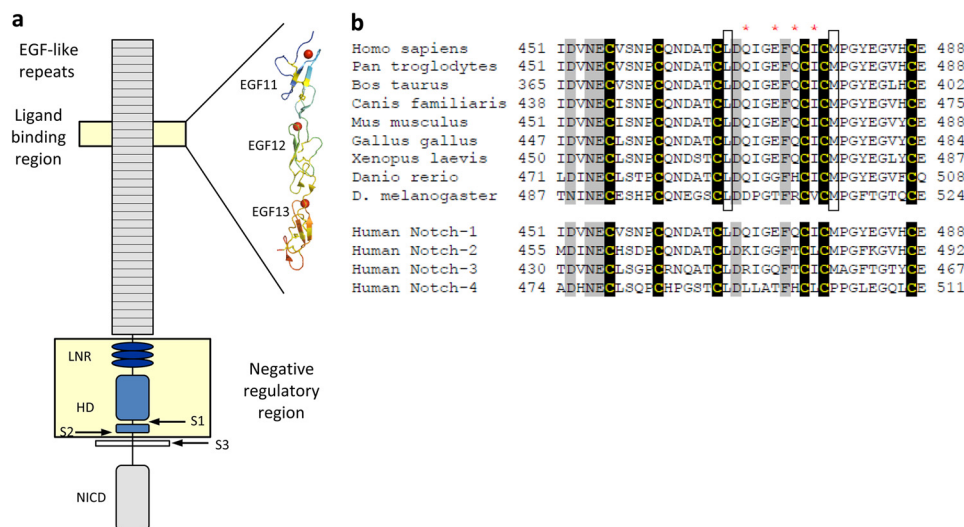
FIGURE 1. **Defining the J-1-binding site in hN-1.** *a*, domain organization of hN-1 showing structure of the hN-1$_{11-13}$ ligand-binding region (Protein Data Bank (PDB) 2VJ3). *LNR,* Lin12-Notch Repeat modules; *HD,* Heterodimerization Domain; *NICD,* Notch Intracellular Domain. *Red spheres* indicate calcium ions. *b*, sequence homology of Notch EGF$_{12}$ region from different species and the four human paralogues; cysteines are shown in *black*, calcium-binding consensus residues are in *gray*, two universally conserved residues that are candidates for ligand binding are *boxed*, and additional residues within the EGF$_{12}$ β-hairpin targeted for mutagenesis are indicated by a *red asterisk*. *D. melanogaster, Drosophila melanogaster.*

ter (BD Biosciences) and FlowJo software (Tree Star). Cytospin cell preparations were incubated with primary antibody for 30 min at room temperature, Notch-1 (A6 mAb, Abcam, dilution 1:200), Notch-2 (goat polyclonal antibody, Abcam, dilution 1:200), Notch-3 (rabbit polyclonal antibody, Abcam, dilution 1:200), Notch-4 (rabbit polyclonal antibody, Abcam, dilution 1:200), or undiluted hybridoma supernatants. After washing in PBS, slides were incubated with secondary antibody, HRP-conjugated goat-anti-mouse antibody (Dako, 1:50 dilution), for murine monoclonal antibodies (mAbs) or with HRP-conjugated goat-anti-rabbit antibody for rabbit polyclonal antibodies (Dako, 1:12.5 dilution) for 30 min at room temperature. Goat antibodies were detected using a mouse-anti-goat monoclonal antibody between primary and secondary antibodies at a 1:12.5 dilution. After washing, color reaction was developed using diaminobenzidine substrate (Dako). Slides were washed and counterstained in hematoxylin before mounting in Aquatex mounting agent (BDH/VWR International).

RESULTS AND DISCUSSION

Site-directed Mutagenesis of Human N-1$_{11-13}$—Mutations in hN-1 were made in the context of the soluble hN-1$_{11-13}$ construct (Fig. 1*a*), which we have previously demonstrated to be ligand binding-competent (19). To assay these hN-1$_{11-13}$ mutants, we have used flow cytometry to study binding to full-length J-1 expressed on the surface of B16 cells. Initially, two mutants containing alanine substitutions were constructed on the basis of sequence conservation across Notch from multiple species (Fig. 1*b*). Of these, one was similar to wild type (WT) in its ability to bind J-1 (M479A), but the other, L468A, was completely unable to bind J-1 (Fig. 2). Mapping Leu-468 to the structure of hN-1$_{11-13}$ shows that it lies within the central β-hairpin of EGF$_{12}$. The Notch-binding region previously identified in the J-1 DSL domain makes it unlikely that Leu-468 is the only residue to contribute to the ligand-binding interface (19); we therefore made a second round of alanine substitutions

at residues that were seen to lie close to this region and to have surface-exposed side chains not involved in calcium coordination (Fig. 1*b*). This allowed us to identify one further mutant, I477A, which abrogated binding similarly to L468A, two other mutants, E473A and Q475A, which showed a more modest reduction in binding, and one mutant, Q470A ,which bound at least as well as WT hN-1$_{11-13}$ (Fig. 2*a*). Loss of binding to L468A and I477A was not due to misfolding or indirect effects on calcium binding (in contrast to a previously studied D469G substitution) because two-dimensional NOESY analysis showed that a marker for calcium binding to EGF$_{12}$ (Tyr-444) gave a similar change in chemical shift upon the addition of Ca^{2+} to that observed in the WT (Fig. 2*b*) (14). The crystal structure of hN-1$_{11-13}$ (PDB 2VJ3) has previously shown that Leu-468 and Ile-477 side chains form a hydrophobic interaction across the central β-hairpin of EGF$_{12}$ (19); our data suggest that this structural feature may serve as a stable platform for ligand interactions (Fig. 2*c*).

Site-directed Mutagenesis of Full-length Drosophila Notch— To extend this analysis to full-length Notch, we then substituted the equivalent amino acids in the evolutionarily distant dN and tested these mutants for interaction with *Drosophila* Serrate using cell aggregation assays. Results were very similar to those seen with the hN-1$_{11-13}$/J-1 interaction, with dN L504A showing the strongest reduction of binding, and as expected, a concomitant reduction in ligand-induced signaling (Fig. 3). An exception was dN V513A, which reduced but did not abrogate binding as had the equivalent hN-1$_{11-13}$ I477A. This most likely reflects the more conservative nature of a valine to alanine change than that of the more bulky isoleucine to alanine. Collectively, our data suggest that the location of the ligand-binding site for the Jagged/Serrate family ligands is conserved across human and *Drosophila* Notch (Table 1) despite the observed sequence divergence within this region (Fig. 1*b*).
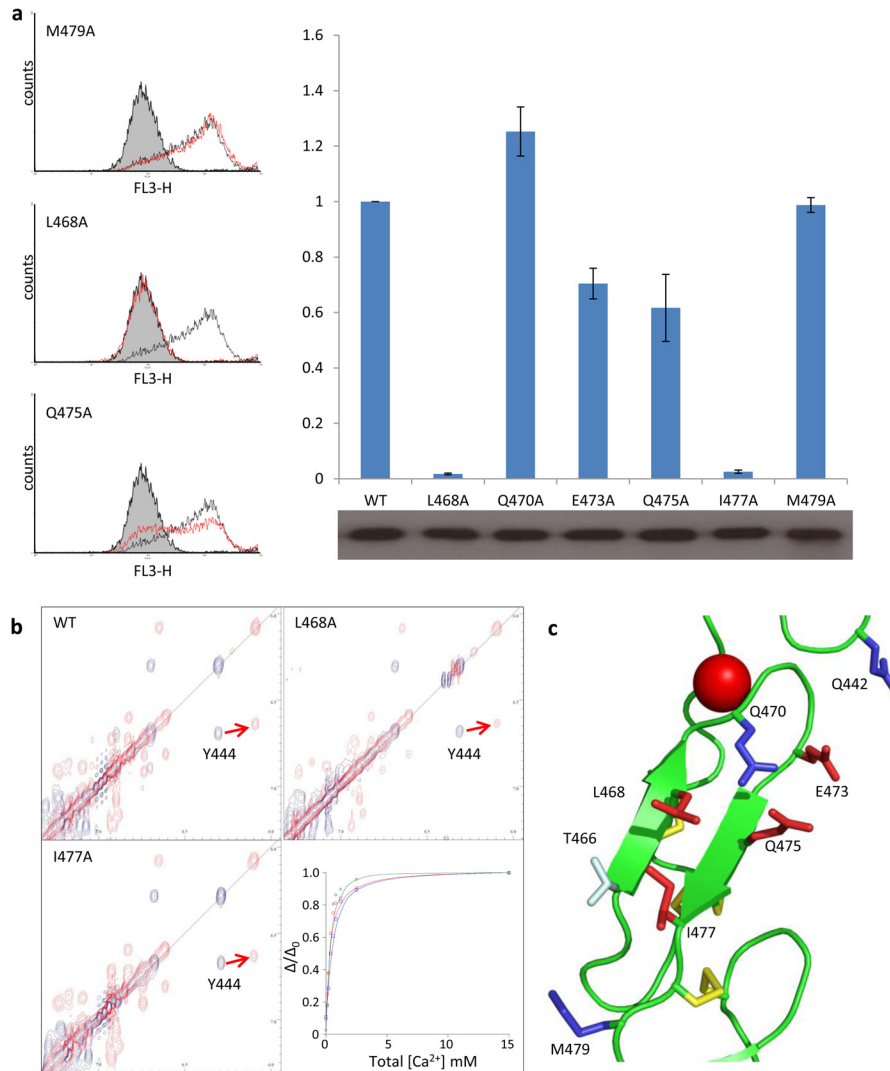
FIGURE 2. **Characterization and interaction studies of hN-1 variants.** *a*, flow cytometry analysis of the interaction between J-1 and biotinylated wild-type (WT) and mutant N-1$_{11-13}$ constructs. *Left-hand panel*, flow cytometry of B16 cells expressing J-1 after interaction with biotinylated hN-1 mutants(*red line*) bound to avidin-coated fluorescent beads (see "Experimental Procedures"); in each case, a negative control (fibrillin calcium-binding EGF$_{12-14}$, *gray shading*) and positive control (WT hN-1$_{11-13}$, *black line*) are shown. Three representative mutant constructs are shown; M479A is indistinguishable from WT, L468A overlays negative control, and Q475A shows intermediate binding. *Right-hand panel*, quantification of flow cytometry data for all EGF$_{12}$ mutants expressed relative to WT control (WT = 1) (*bars* indicate mean, *error bars* indicate S.D., $n \geq 3$) and Western blot of hN-1$_{11-13}$ samples to show experiments controlled for protein loading. *b*, NMR analysis shows that WT and mutant constructs have native-like calcium binding properties indicative of correct folding. Aromatic regions of ^{1}H-^{1}H two-dimensional NOESY spectra at pH 7.5 of hN-1$_{11-13}$ WT, L468A, and I477A are shown. A marker for calcium binding in EGF$_{12}$ (Tyr-444) is highlighted in the absence (*blue*) and presence (*red*) of Ca^{2+} (15 mM), and the shift is indicated by a *red arrow*. Quantification of data indicates relative chemical shift change on addition of Ca^{2+}. *Red*, WT; *blue*, L468A; *green*, I477A. The structure of hN-1 EGF$_{12}$ (PDB 2VJ3) is shown; residues implicated in binding by flow cytometry (*red*), non-binding residues (*blue*), position of residue Thr-466 that is implicated in regulation by *O*-fucosylation, and Fringe extension are indicated.

These mutational data now implicate a different face of Notch in ligand binding from our earlier studies based on NMR data derived from mapping intensity changes in the spectrum of hN-1$_{11-13}$ upon titration of an hJ-1$_{DSL-EGF3}$ fragment (19) (the more informative chemical shift mapping was not possible due to a combination of the poor solubility of hJ-1$_{DSL-EGF3}$ and the kinetics/affinity of the interaction). The most perturbed residues in this assay were hN-1 Val-453 and Gly-472, which contribute to the EGF$_{12}$ calcium binding by donation of a backbone carbonyl ligand and to an EGF$_{11-12}$ packing interaction, respectively. The spatial distance and orientation of Val-453 and Gly-472, when compared with the Leu-468 and Ile-477 hydrophobic patch identified as being important for ligand binding in this study, preclude both sites making direct con-

tacts to the ligand. To try and resolve this contradiction, we mutated the Val-453 equivalent residue, Ile-489, in dN. This had no effect on ligand binding (data not shown), implying that the intensity changes observed previously (19) reflect an indirect effect on the residues stabilizing calcium binding to EGF$_{12}$ by ligand binding within the central β-hairpin (because β-hairpin stability and calcium binding affinity are closely coupled).

This conservation of ligand-binding site between human and evolutionary distant *Drosophila* Notch proteins, despite a relatively high level of sequence diversity (Fig. 1*b*) and differences in the specific ligands assayed, suggests that this region of Notch will be involved in ligand binding in all species. It is also interesting to note that the threonine/serine residue (Thr-466 in hN-1$_{11-13}$/Ser-502 in dN), implicated in the regula-

tion of Notch activity by *O*-fucosylation and subsequent Fringe extension, lies adjacent to the ligand-binding patch revealed in EGF_{12} (Fig. 2*c*), suggesting that direct effects on ligand recognition may explain the functional effects of this modification (25, 26).

Sequence Variation in Notch Paralogues—Inspection of the amino acid sequences of residues in the vicinity of our newly defined Notch ligand-binding site across mammalian Notch paralogues (human Notch 1–4 shown) reveals sequence variation (Fig. 1*b*), as we have observed between hN-1 and *Drosophila* Notch. Our binding data for human N-1 show that alanine substitution of residues in close proximity to the core binding site can subtly enhance or reduce ligand binding (Fig. 2*a*). One explanation for the sequence variation seen in such a functionally important site therefore is to allow fine tuning of the affinity, specificity, and regulation of different Notch-ligand combi-

nations (there are five ligands and four Notch receptors in mammals). This is consistent with data from various assays that have demonstrated that hNotch paralogues 1–3 can all interact with both J-1 and Dll-1 (7, 14, 27–29). All paralogues maintain the leucine-isoleucine, or leucine-leucine, pairings predicted on the basis of structural homology with hN-1 to form the ligand-binding platform. It is also interesting to note that *Xenopus* Notch (Xotch) (which has an identical β-hairpin sequence between C^3 and C^5 in EGF_{12} to hN-1 (Fig. 1*b*)) has been observed to bind to *Drosophila* ligands Serrate and Delta (6). A potential consequence of the observed variability in the binding site is to allow generation of paralogue-specific antibodies that block ligand binding.

Production of Paralogue-specific Antibodies—To test our hypothesis, we have used our soluble $hN-1_{11–13}$ containing the ligand-binding site to generate a panel of mAbs. Of these, one mAb (N1-39E) is seen to block receptor/ligand complex formation between $hN-1_{11–13}$ and cell surface expressed J-1 in our flow cytometry assay, whereas another mAb N1-96A has no effect on the interaction (Fig. 4*a*). Epitope mapping localizes the binding site of both N1-39E and N1-96A to EGF_{12} and/or the C-terminal region of EGF_{11} because they both recognize hN-1 mutants defective in calcium binding to EGF_{11} and EGF_{13}, but do not recognize a mutant defective in calcium binding to EGF_{12} (Fig. 4*b*). Subsequent testing against our panel of hN-1 EGF_{12} mutants demonstrates that the epitope of N1-39E, but not N1-96A, encompasses residues 468–477 of hN-1, which includes Leu-468 and Ile-477, directly implicated above in ligand binding, and Gln-470, Glu-473, and Gln-475 (Fig. 4*c*). The N1-39E epitope thus lies within the EGF_{12} Notch ligand-recognition site, explaining the molecular mechanism underlying its blockade of the hN-1/J-1 interaction. To test whether or not N1-39E is paralogue-specific, as suggested by the residues that form its epitope (Figs. 1*b* and 4*c*), we assayed whether or not it could recognize HEK 293 cells transfected individually with the different hNotch paralogues (N-1, N-2, N-3, and N-4). Flow cytometry analysis demonstrated that N1-39E specifically recognized only HEK293 cells expressing N-1 (expression of hNotch by each transfected cell line was confirmed by immunocytochemistry (Fig. 4*d*)). Recent work has demonstrated that selective interference of Notch paralogue activity by antibody binding can inhibit tumor growth in mouse xenograft models with reduced intestinal toxicity (30). Such reagents are likely to be valuable in the treatment of
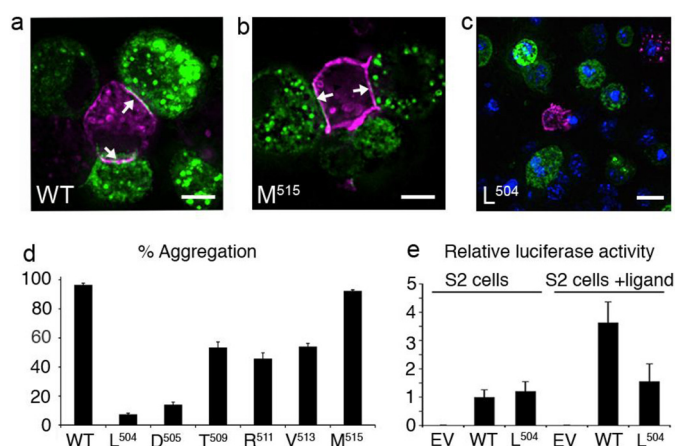
FIGURE 3. **Defining the ligand-binding site in dN.** *a–c*, cell aggregation assay of the interaction of full-length Serrate with WT and alanine substitution mutants of full-length dN expressed in S2 cells. Panels show merged immunofluorescence images of Serrate (*purple*), Notch (*green*), and DAPI (*blue*). Aggregated cells form junctions with clustered Serrate and Notch indicated by *arrows*, which are clearly evident for WT Notch (*a*) and the M515A mutant (*b*) but not for the L504A construct (*c*). The latter is shown at lower magnification to depict a field of nonaggregating cells. *Scale bars* are: 5 μm (*a* and *b*) and 10 μm (*c*). *d*, cell aggregation assay scored as the percentage of Notch-expressing cells adhered to at least one Serrate-expressing cell for WT dN, the control D505A substitution, and for substitutions located around the main β-sheet of EGF_{12}. *Error bars* in *d* indicate S.D., $n \geq 3$. *e*, Notch luciferase-reporter signaling assay. Mean normalized Notch signaling is shown relative to WT Notch expressed in S2 cells co-cultured with nonexpressing S2 cells. Signaling through wild-type Notch is increased by ligand-expressing (Delta) co-cultured S2 cells, but signaling through L504A mutant is not changed by exposure to ligand. *EV*, empty vector-transfected luciferase reporter controls. *Error bars* in *e* indicate S.D., $n = 6$.

TABLE 1

Site-directed mutagenesis of residues in hN-1 and *Drosophila* Notch and their respective effects in flow cytometry, ligand binding, and cell aggregation assays

ND, not determined.

| hN-1 residue and substitution	EGF domain	Effect on ligand binding observed in flow cytometry analysis	Equivalent substitution in *Drosophila* Notch	Effect on Notch/Serrate cell aggregation
Q442A[a]	11	Binds as WT	Q478A	Close to WT level
L468A	12	No binding	L504A	Strongly reduced
D469G[b]	12	No binding	D505A	Strongly reduced
Q470A	12	Binds as WT	ND	ND
E473A	12	Moderate binding	T509A	Moderately reduced
Q475A	12	Moderate binding	R511A	Moderately reduced
I477A	12	No binding	V513A	Moderately reduced
M479A	12	Binds as WT	M515A	Binds as WT

[a] Gln-442 in EGF_{11} is in close proximity to the region of ligand binding in EGF_{12}.
[b] Conserved calcium-binding residue. Loss of ligand binding is due to loss in structural integrity, rather than direct involvement in N-1/ligand interaction.
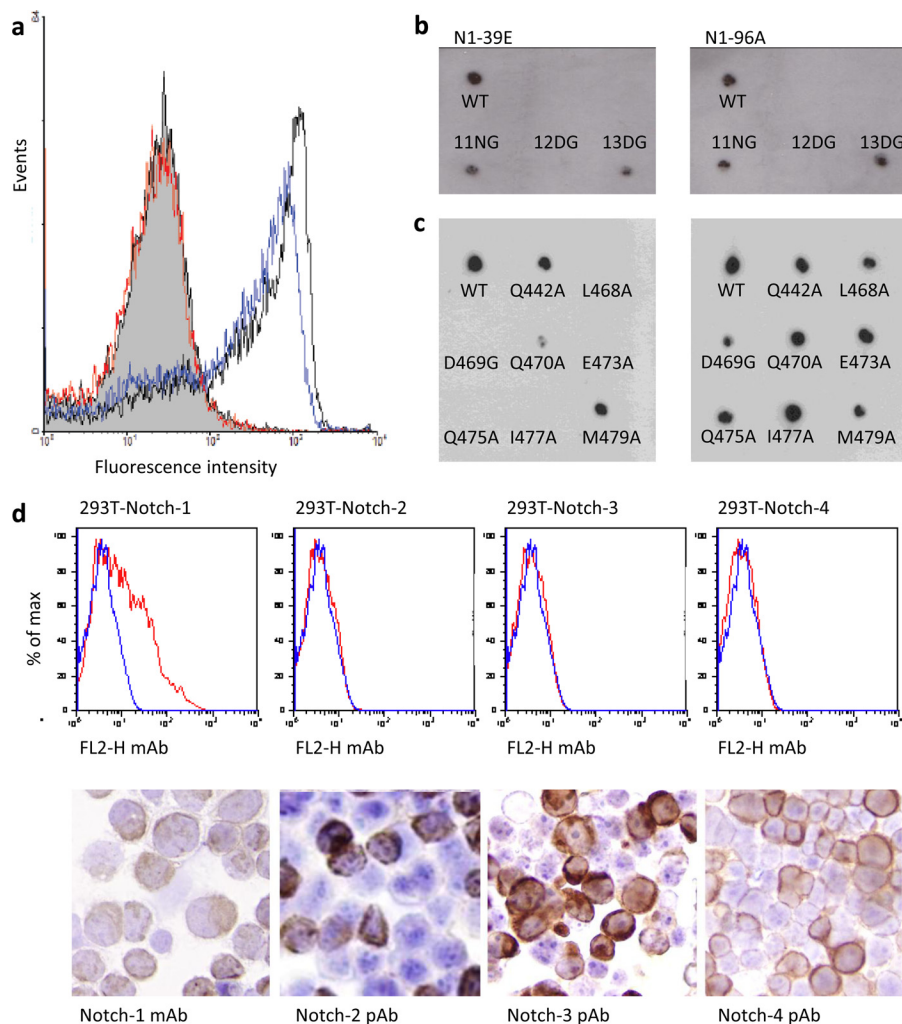
FIGURE 4. **Characterization of a ligand-blocking mAb to hN-1, which recognizes J-1-binding site.** *a*, flow cytometry assay to show mAb N1-39E (*red*), but not N1-96A (*blue*), blocks the binding of hN-1$_{11-13}$ to HEK cells expressing hJ-1. *b* and *c*, epitope mapping by dot-blotting of WT and mutant hN-1$_{11-14}$ proteins (11NG, 12DG, 13DG) that contain a calcium-binding mutation in EGF$_{11}$, EGF$_{12}$, or EGF$_{13}$ localizes the epitope of mAb N1-39E and N1-96A to EGF$_{12}$ or the C terminus of EGF$_{11}$. Dot-blotting of a panel of hN-1 EGF$_{12}$ mutants demonstrates that L468A, Q470A, E473A, Q475A, and I477A are not recognized by N1-39E, and thus form part of its epitope. *d*, flow cytometry and immunocytochemistry (cytospin) analysis demonstrates that N1-39E is paralogue-specific. The *red line* indicates binding of mAb N1-39E; only 293T cells expressing hN-1 show a positive result, indicated by a rightward shift. Cytospin analysis (using monoclonal (*mAb*) or polyclonal (*pAb*) paralogue-specific antibodies) shows that each transfected cell line tested expresses a specific human Notch paralogue.
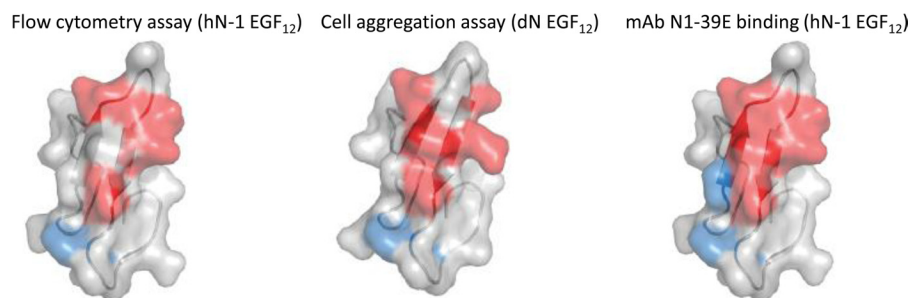
FIGURE 5. **Amino acid residues within β-hairpin implicated in ligand recognition and antibody binding in human and *Drosophila* Notch.** EGF$_{12}$ of hN-1 is shown as a graphic and overlaid with a *semitransparent surface*. Positions that perturb activity in an assay are colored in *red*, those with no effect are colored in *blue*, and those not probed are colored in *gray*.

breast, melanoma, and T-cell acute lymphoblastic leukemia cancers, which are associated with aberrant Notch signaling, as well as important research tools (31). To date, potential therapeutic antibodies have targeted the negative regulatory region of Notch and have shown activity against Notch-1, -2, and -3 (30, 32, 33); antibodies to the extracellular domain of hN-1 encompassing EGF$_{1-13}$ and EGF$_{11-15}$ have also been reported (33, 34). We have now demonstrated a strategy for producing paralogue-specific antibodies to a region known to be critical for ligand binding. It should be noted that monoclonal antibodies raised to the ligand-binding region of Notch, and which block binding, may or may not reduce signaling (34, 35). This is

most likely due to the different affinities of the antibodies, their ability to recognize post-translationally modified forms of the receptor, or the cells used in the signaling assay expressing more than one paralogue on the cell surface. Nevertheless, given appropriate scale-up and screening of the molecular properties of such antibodies, this approach should yield reagents important for future research and therapeutics.

Our data demonstrate that the position and hydrophobic nature of the binding site for Jagged/Serrate ligands is conserved on the Notch EGF_{12} molecular surface throughout evolution (Fig. 5). Despite such global conservation, individual differences within the EGF_{12} site occur, suggesting that fine-tuning of the receptor/ligand interaction is possible, which may be subject to further regulation by *O*-glycosylation. As a consequence of the sequence variation observed, we demonstrate that it is possible to make targeted paralogue-specific, ligand-blocking mAbs (Fig. 5), which may be important for future research and therapeutics.

REFERENCES

1. Artavanis-Tsakonas, S., Rand, M. D., and Lake, R. J (1999) Notch signaling: cell fate control and signal integration in development. *Science* **284,** 770 –776
2. Hansson, E. M., Lendahl, U., and Chapman, G. (2004) Notch signaling in development and disease. *Semin. Cancer Biol.* **14,** 320 –328
3. Blaumueller, C. M., Qi, H., Zagouras, P., and Artavanis-Tsakonas, S. (1997) Intracellular cleavage of Notch leads to a heterodimeric receptor on the plasma membrane. *Cell* **90,** 281 –291
4. Sanchez-Irizarry, C., Carpenter, A. C., Weng, A. P., Pear, W. S., Aster, J. C., and Blacklow, S. C. (2004) Notch subunit heterodimerization and prevention of ligand-independent proteolytic activation depend, respectively, on a novel domain and the LNR repeats. *Mol. Cell. Biol.* **24,** 9265 –9273
5. Fleming, R. J. (1998) Structural conservation of Notch receptors and ligands. *Semin. Cell Dev. Biol.* **9,** 599 – 607
6. Rebay, I., Fleming, R. J., Fehon, R. G., Cherbas, L., Cherbas, P., and Artavanis-Tsakonas, S. (1991) Specific EGF repeats of Notch mediate interactions with Delta and Serrate: implications for Notch as a multifunctional receptor. *Cell* **67,** 687 – 699
7. Shimizu, K., Chiba, S., Kumano, K., Hosoya, N., Takahashi, T., Kanda, Y., Hamada, Y., Yazaki, Y., and Hirai, H. (1999) Mouse Jagged1 physically interacts with Notch2 and other Notch receptors: assessment by quantitative methods. *J. Biol. Chem.* **274,** 32961 –32969
8. Brou, C., Logeat, F., Gupta, N., Bessia, C., LeBail, O., Doedens, J. R., Cumano, A., Roux, P., Black, R. A., and Israël, A. (2000) A novel proteolytic cleavage involved in Notch signaling: the role of the disintegrin-metalloprotease TACE. *Mol. Cell* **5,** 207 –216
9. Nichols, J. T., Miyamoto, A., Olsen, S. L., D'Souza, B., Yao, C., and Weinmaster, G. (2007) DSL ligand endocytosis physically dissociates Notch1 heterodimers before activating proteolysis can occur. *J. Cell Biol.* **176,** 445 – 458
10. Parks, A. L., Klueg, K. M., Stout, J. R., and Muskavitch, M. A. (2000) Ligand endocytosis drives receptor dissociation and activation in the Notch pathway. *Development* **127,** 1373 –1385
11. Mumm, J.S., Schroeter, E. H., Saxena, M. T., Griesemer, A., Tian, X., Pan, D. J., Ray, W. J., and Kopan, R. (2000) A ligand-induced extracellular cleavage regulates γ-secretase-like proteolytic activation of Notch1. *Mol. Cell* **5,** 197 –206
12. Schroeter, E. H., Kisslinger, J. A., and Kopan, R. (1998) Notch-1 signalling requires ligand-induced proteolytic release of intracellular domain. *Nature* **393,** 382 –386
13. Jarriault, S., Brou, C., Logeat, F., Schroeter, E. H., Kopan, R., and Israel, A. (1995) Signalling downstream of activated mammalian Notch. *Nature* **377,** 355 –358
14. Cordle, J., Redfield, C., Stacey, M., van der Merwe, P. A., Willis, A. C., Champion, B. R., Hambleton, S., and Handford, P. A. (2008) Localization of the Delta-like-1-binding site in human Notch-1 and its modulation by calcium affinity. *J. Biol. Chem.* **283,** 11785 –11793
15. Fehon, R. G., Kooh, P. J., Rebay, I., Regan, C. L., Xu, T., Muskavitch, M. A., and Artavanis-Tsakonas, S. (1990) Molecular interactions between the protein products of the neurogenic loci *Notch* and *Delta*, two EGF-homologous genes in *Drosophila*. *Cell* **61,** 523 –534
16. Harris, R. J., van Halbeek, H., Glushka, J., Basa, L. J., Ling, V. T., Smith, K. J., and Spellman, M. W. (1993) Identification and structural analysis of the tetrasaccharide NeuAc $\alpha(2\rightarrow6)$Gal $\beta(1\rightarrow4)$GlcNAc $\beta(1\rightarrow3)$Fuc $\alpha 1\rightarrow O$-linked to serine 61 of human factor IX. *Biochemistry* **32,** 6539 – 6547
17. Panin, V. M., Shao, L., Lei, L., Moloney, D. J., Irvine, K. D., and Haltiwanger, R. S. (2002) Notch ligands are substrates for protein *O*-fucosyltransferase-1 and Fringe. *J. Biol. Chem.* **277,** 29945 –29952
18. Hicks, C., Johnston, S. H., diSibio, G., Collazo, A., Vogt, T. F., and Weinmaster, G. (2000) Fringe differentially modulates Jagged1 and Delta1 signalling through Notch1 and Notch2. *Nat. Cell Biol.* **2,** 515 –520
19. Cordle, J., Johnson, S., Tay, J. Z., Roversi, P., Wilkin, M. B., de Madrid, B. H., Shimizu, H., Jensen, S., Whiteman, P., Jin, B., Redfield, C., Baron, M., Lea, S. M., and Handford, P. A. (2008) A conserved face of the Jagged/Serrate DSL domain is involved in Notch trans-activation and cis-inhibition. *Nat. Struct. Mol. Biol.* **15,** 849 – 857
20. Handford, P. A., Baron, M., Mayhew, M., Willis, A., Beesley, T., Brownlee, G. G., and Campbell, I. D. (1990) The first EGF-like domain from human factor IX contains a high-affinity calcium binding site. *EMBO J.* **9,** 475 – 480
21. Suk, J. Y., Jensen, S., McGettrick, A., Willis, A. C., Whiteman, P., Redfield, C., and Handford, P. A. (2004) Structural consequences of cysteine substitutions C1977Y and C1977R in calcium-binding epidermal growth factor-like domain 30 of human fibrillin-1. *J. Biol. Chem.* **279,** 51258 –51265
22. Fleming, R. J., Scottgale, T. N., Diederich, R. J., and Artavanis-Tsakonas, S. (1990) The gene Serrate encodes a putative EGF-like transmembrane protein essential for proper ectodermal development in *Drosophila melanogaster*. *Genes Dev.* **4,** 2188 –2201
23. Bunch, T. A., Grinblat, Y., and Goldstein, L. S. (1988) Characterization and use of the *Drosophila* metallothionein promoter in cultured *Drosophila melanogaster* cells. *Nucleic Acids Res.* **16,** 1043 –1061
24. Mason, D., Cordell, J., and Pulford, K.. (1983) Production of monoclonal antibodies for immunocytochemical use. in *Techniques in Immunocytochemistry*, Vol 2 (Bullock, G. R., and Petrusz, P., eds) pp. 175–216. London Academic Press Ltd., London, UK
25. Panin, V. M., Papayannopoulos, V., Wilson, R., and Irvine, K. D. (1997) Fringe modulates Notch-ligand interactions. *Nature* **387,** 908 –912
26. Moloney, D. J., Panin, V. M., Johnston, S. H., Chen, J., Shao, L., Wilson, R., Wang, Y., Stanley, P., Irvine, K. D., Haltiwanger, R. S., and Vogt, T. F. (2000) Fringe is a glycosyltransferase that modifies Notch. *Nature* **406,** 369 –375
27. Hofmann, J. J., Zovein, A. C., Koh, H., Radtke, F., Weinmaster, G., and Iruela-Arispe, M. L. (2010) Jagged1 in the portal vein mesenchyme regulates intrahepatic bile duct development: insights into Alagille syndrome. *Development* **137,** 4061 – 4072
28. Shimizu, K., Chiba, S., Saito, T., Kumano, K., Takahashi, T., and Hirai, H. (2001) Manic fringe and lunatic fringe modify different sites of the Notch2 extracellular region, resulting in different signaling modulation. *J. Biol. Chem.* **276,** 25753 –25758
29. Peters, N., Opherk, C., Zacherle, S., Capell, A., Gempel, P., and Dichgans, M. (2004) CADASIL-associated Notch3 mutations have differential effects both on ligand binding and ligand-induced Notch3 receptor signaling through RBP-Jk. *Exp. Cell Res.* **299,** 454 – 464
30. Wu, Y., Cain-Hom, C., Choy, L., Hagenbeek, T. J., de Leon, G. P., Chen, Y., Finkle, D., Venook, R., Wu, X., Ridgway, J., Schahin-Reed, D., Dow, G. J., Shelton, A., Stawicki, S., Watts, R. J., Zhang, J., Choy, R., Howard, P.,

Kadyk, L., Yan, M., Zha, J., Callahan, C. A., Hymowitz, S. G., and Siebel, C. W. (2010) Therapeutic antibody targeting of individual Notch receptors. *Nature* **464,** 1052–1057

31. Weng, A. P., Ferrando, A. A., Lee, W., Morris, J. P., 4th, Silverman, L. B., Sanchez-Irizarry, C., Blacklow, S. C., Look, A. T., and Aster, J. C. (2004) Activating mutations of NOTCH1 in human T cell acute lymphoblastic leukemia. *Science* **306,** 269–271

32. Li, K., Li, Y., Wu, W., Gordon, W. R., Chang, D. W., Lu, M., Scoggin, S., Fu, T., Vien, L., Histen, G., Zheng, J., Martin-Hollister, R., Duensing, T., Singh, S., Blacklow, S. C., Yao, Z., Aster, J. C., and Zhou, B. B. (2008) Modulation of Notch signaling by antibodies specific for the extracellular negative regulatory region of NOTCH3. *J. Biol. Chem.* **283,** 8046–8054

33. Aste-Amézaga, M., Zhang, N., Lineberger, J. E., Arnold, B. A., Toner, T. J., Gu, M., Huang, L., Vitelli, S., Vo, K. T., Haytko, P., Zhao, J. Z., Baleydier, F., L'Heureux, S., Wang, H., Gordon, W. R., Thoryk, E., Andrawes, M. B., Tiyanont, K., Stegmaier, K., Roti, G., Ross, K. N., Franlin, L. L., Wang, H., Wang, F., Chastain, M., Bett, A. J., Audoly, L. P., Aster, J. C., Blacklow, S. C., and Huber, H. E. (2010) Characterization of Notch1 antibodies that inhibit signaling of both normal and mutated Notch1 receptors. *PLoS One* **5,** e9094

34. Sharma, A., Paranjape, A. N., Rangarajan, A., and Dighe, R. R. (2012) A monoclonal antibody against human Notch1 ligand binding domain depletes subpopulation of breast cancer stem-like cells. *Mol. Cancer Ther.* **11,** 77–86

35. Falk, R., Falk, A., Dyson, M. R., Melidoni, A. N., Parthiban, K., Young, J. L., Roake, W., McCafferty, J. (2012) Generation of anti-Notch antibodies and their application in blocking Notch signalling in neural stem cells. *Methods* **58,** 69–78

Molecular Basis for Jagged-1/Serrate Ligand Recognition by the Notch Receptor

Pat Whiteman, Beatriz Hernandez de Madrid, Paul Taylor, Demin Li, Rebecca Heslop,
Nattnee Viticheep, Joyce Zi Tan, Hideyuki Shimizu, Juliana Callaghan, Massimo
Masiero, Ji Liang Li, Alison H. Banham, Adrian L. Harris, Susan M. Lea, Christina
Redfield, Martin Baron and Penny A. Handford

Access the most updated version of this article at doi: 10.1074/jbc.M112.428854

Alerts:
- When this article is cited
- When a correction for this article is posted

Click here to choose from all of JBC's e-mail alerts

This article cites 35 references, 14 of which can be accessed free at
http://www.jbc.org/content/288/10/7305.full.html#ref-list-1